Analysis of Offshore Foundations Subjected to Storm Loading

Hossein A. Taiebat
Centre for Geotechnical Research, The University of Sydney

Summary: The potential for liquefaction of seabed sand underneath an offshore foundation subjected to cyclic storm loading is investigated. A semi-analytical approach has been adopted in the formulation of three dimensional finite element method for consolidation analysis. The effects of densification due to cyclic loading are also considered in the formulation. Results of experimental studies on sand samples are used to evaluate the effect of cyclic loading at different points in the soil. As an illustration of the method, the possibility of liquefaction of calcareous sand around a hypothetical offshore foundation under storm loading is investigated.

1 INTRODUCTION

The stability of foundations for offshore structures can be strongly affected if the seabed sediments have the potential to liquefy under wave-induced cyclic loading. The potential for liquefaction of seabed soils, particularly loose sands, is therefore a major issue that should be considered by the designers of offshore facilities on granular materials.

Foundations of marine structures are generally subjected to two kinds of loadings; ambient loads due to submerged weight and cyclic loads due to waves applied during a storm. Cyclic loads include a large number of cycles of short to medium periods (*5* to *15sec.*). Laboratory tests on sands have shown that the application of a large number of cyclic loads with moderate amplitude could produce a progressive degradation of the soil resistance and buildup of pore water pressures, which can alter the stability of marine structures founded on such soil. The pore pressure at various places within the soil profile may build up to a stage where it becomes equal to the mean effective stress resulting in cyclic liquefaction and leading to possible instability.

1.1 Liquefaction phenomena

The most important feature of cyclic loading on sands is the cumulative densification which is responsible for such phenomena as liquefaction and loss of strength. Numerous experiments on various sands show that cyclic stresses or strains cause slip at grain to grain contacts. This inter-granular slip, in dry sands, would lead to volumetric compaction. In saturated sands where the drainage path is long or cyclic loads are applied at high frequencies, the volumetric compaction is retarded because water can not drain instantaneously to accommodate the volume change. Consequently, the sand skeleton transfers some of its inter-granular or effective stresses to the pore water and the pore water pressures increase. Reduction in effective stresses leads to a structural rebound in the sand skeleton and reduces shearing resistance of the soil. In extreme cases, the pore water pressure developed during cyclic loading may increase until all the inter-granular or effective stresses acting on the soil skeleton are eliminated from the system. In this case the soil flows like a viscous liquid and liquefaction is said to have occurred (Finn *et al*, 1976).

1.2 Experimental studies of liquefaction

In laboratory undrained tests, liquefaction is characterized by a rise in pore water pressure to a value equal to the consolidation pressure in triaxial tests or to the initial vertical stress in simple shear tests. Excessive strains accompany the high pore water pressure rise and the sample collapses within a few cycles after the pore pressure becomes equal to the initial consolidation stress.

The knowledge of pore pressure response to a cyclic loading and its interaction with the soil skeleton is an important feature for a liquefaction analysis. The results of experimental tests on saturated sand are usually expressed in term of the number of cycles required for liquefaction, N_l, under various levels of cyclic stress ratio, q_{cyc}/p', where q_{cyc} is the cyclic deviatoric stress applied to the sample and p' is the mean consolidation stress. Typical results of experimental studies which were conducted on samples of calcareous sand under cyclic loading and undrained conditions (Kaggwa, 1988) are presented in Fig. 1.

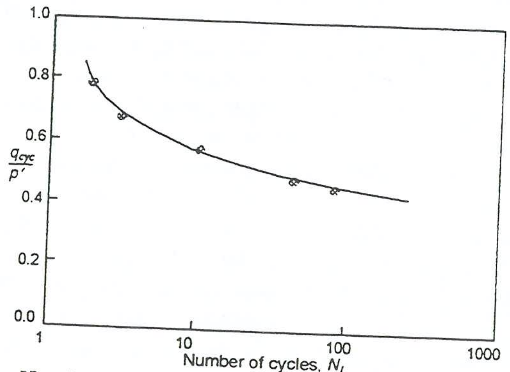

Fig. 1 : Number of cycles required for liquefaction versus cyclic stress ratio

The rate of pore pressure generation is usually related to the cyclic ratio, N/N_l, by a pore pressure generation function (Seed and Idriss, 1982). The rate of pore pressure generation can be expressed as :

$$\frac{u_g}{p'} = \frac{2}{\pi} Arc\sin\left(\frac{N}{N_l}\right)^{1/2\theta} \quad (1)$$

where u_g is the pore pressure developed due to cyclic loading, N is the number of stress cycles applied to the sample, and θ is a factor related to the type of material and the magnitude of initial deviatoric stress, q. A value of θ was proposed by Kaggwa (1988) for calcareous sands as:

$$\theta = 1.68\, e^{6.79q/p'} \quad (2)$$

A family of curves which represent the pore pressure generation function with different values of θ is plotted in Fig. 2.

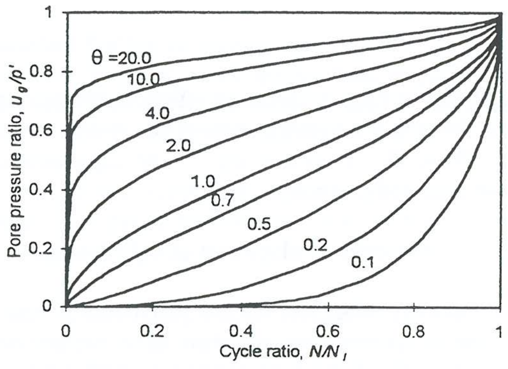

Fig. 2 : Rate of pore pressure generation for various θ

1.3 Evaluation of liquefaction of soils under foundations

Application of cyclic loading to a foundation will also generate pore pressures in the soil. However, the net increase in pore pressure will be the resultant of the pore pressure generation due to cyclic loading, the diffusion of pore pressure within the soil, and the dissipation of the pore pressure through drainage boundaries.

Development of pore pressures and strains resulting from cyclic loading can be predicted mainly by two numerical approaches. The first one is an incremental analysis in which the whole stress path is followed for every individual load cycle by using a hysteritic stress-strain relationship. Application of this method for evaluation of liquefaction in the field is not practical since it requires a large computational effort. In the second approach, the tendency to accumulate strain and its subsequent effects on pore pressure generation are considered at the end of one or more cycles. The results of physical experiments are used to correlate the accumulation of strain and pore pressure due to cyclic loading. Depending on the availability and level of sophistication of experimental and numerical tools, various methods for liquefaction analysis have been developed. Most of the studies on liquefaction potential of offshore foundations are based on the second approach, some of them are summarized below.

One of the earliest evaluations of the possibility of liquefaction was performed by Bjerrum (1973). Based on results of undrained simple shear tests, he estimated the excess pore pressure increment of every single wave and determined the excess pore pressure at the end of a storm by summing up the pore pressure increments. The effect of dissipation of pore water pressure during the storm was ignored. Lee and Focht (1975) consider the effect of pore pressure dissipation in a pragmatic manner by modifying the experimental procedure.

Rahman *et al* (1977) presented a more rigorous solution to the problem by considering the effects of stress distribution in the soil profile and dissipation of pore pressure using a finite element analysis based on Darcy's Law. Chugh and Thun (1985) used the same procedure for one dimensional dynamic analysis of a liquefiable soil. In both methods, the stress distribution in the soil profile was obtained from independent sources.

Reese *et al* (1988) analysed a pile subjected to lateral load generated by storm waves. The results of strain-control cyclic tests on sand samples were used to calculate the pore pressure. The deflection of the pile due to lateral load was obtained using the p-y method. The strain field was calculated by employing a "hybrid, finite-element-type formulation". The dissipation of pore pressure was then evaluated using an axi-symmetric finite element model.

1.4 Procedure for analysis of liquefaction

A procedure for the analysis of liquefaction based on the second approach is used in this study. The procedure incorporates the generation of pore water pressure due to cyclic loading under undrained conditions, followed by an analysis of pore pressure dissipation both during and after a storm event. Experimental test data on the sand are used to evaluate the pore water pressure generated at any point in the soil during cyclic loading.

The analysis includes a number of steps, viz.
1-definition of storm and the resulting loads that act on the foundation,
2-computation of initial and cyclic stresses within the soil,
3-estimation of excess pore water pressures resulting from the cyclic loading under undrained conditions,
4-incorporation of the cyclic load effects in a finite element program and solving for dissipation of pore water pressures.

2 NUMERICAL FORMULATION

The three dimensional nature of the stress and strain fields in the soil under a foundation subjected to lateral cyclic loading is one of the main difficulties in a liquefaction analysis. A numerical tool is required, capable of performing a three dimensional consolidation analysis. The numerical tool should be efficient and quick, because in a liquefaction analysis, the whole process of generation and dissipation of pore water pressure must be followed thousands of times during a storm.

In the present paper, the procedure described in section 1.4 is used to analyse the possibility of liquefaction in soil. A unique feature of the analysis is that the effect of excess pore pressure is explicitly taken into account. An efficient finite element program has been developed based on a semi-analytical approach (Zienkiewicz and Taylor, 1989). The method presented originally by Zienkiewicz *et al* (1982) has been used to include an additional accumulation of strain due to cyclic loading into the finite element formulation.

2.1 Effects of cyclic loads

The cyclic loading on saturated sands can be viewed as an agency that causes a reorientation and repositioning of sand particles, which leads to a reduction in void spaces. As a consequence, in an undrained test, water pressure in the voids rises and in a drained test, displacement and volumetric strain increase. The change in the void spaces due to cyclic loading can be considered as a change in strain, $d\varepsilon^c$, within the samples.

A reasonable approximation to the cyclic strain generated by cyclic load, $d\varepsilon^c$, is to consider it to be isotropic, i.e.:

$$d\varepsilon^c = e.d\varepsilon_v^c/3 \tag{3}$$

where $d\varepsilon_v^c$ is the change in the volumetric strain due to the change in the voids volume, and $e=(1,1,1,0,0,0)^T$.

The total strain, $d\varepsilon^t$, can be regarded as the sum of strain changes related directly to stresses, $d\varepsilon^s$, and strain changes which are generated by cyclic loads, $d\varepsilon^c$, i.e.

$$d\varepsilon^t = d\varepsilon^s + d\varepsilon^c \tag{4}$$

The general stress-strain relationship can be given as:

$$d\sigma' = \boldsymbol{D}(d\varepsilon^t - d\varepsilon^c) \tag{5}$$

in which $\boldsymbol{D}$ is the stiffness matrix of the solid skeleton.

The definitions of effective and total stresses and their link with pore pressure gives:

$$d\sigma = d\sigma' + e.du \tag{6}$$

where $d\sigma$ denotes the change in total stress in the soil, and u is the excess pore water pressure.

Substituting equations (3) and (6) into equation (5) yields:

$$d\varepsilon^t = e.d\varepsilon_v^c/3 + \boldsymbol{D}^{-1}(d\sigma - e.du) \tag{7}$$

For an undrained test, $e^T.d\varepsilon^t = 0$, and in such tests where the average stress level is held constant, $d\sigma = 0$, the pore water pressure will rises to du_g due to cyclic loading. Therefore equation (7) gives:

$$d\varepsilon_v^c = e^T.\boldsymbol{D}^{-1}.e.du_g \tag{8}$$

where du_g represents the pore pressure generated by cyclic loading alone.

Equation (8) relates the pore pressure generated in an undrained cyclic test to the volumetric strain in a drained cyclic test. By this expression the volumetric strain and the pore water pressure can interchangeably be used in all computations (provided the inverse of $\boldsymbol{D}$ can be evaluated). The use of the latter is convenient as it represents the most direct connection between the experimental data and subsequent calculations.

Substituting equation (8) in (7) results in a general stress-strain relationship that can be used in the formulation of finite element method, i.e.

$$d\varepsilon^t = e.e^T.\boldsymbol{D}^{-1}.e.du_g/3 + \boldsymbol{D}^{-1}(d\sigma - e.du) \tag{9}$$

or in a more general form:

$$d\sigma - e.du = \boldsymbol{D}.d\varepsilon^t - \boldsymbol{D}.\,d\varepsilon^c \tag{10}$$

in which:

$$d\varepsilon^c = e.e^T.\boldsymbol{D}^{-1}.e.du_g/3 \tag{11}$$

Computationally, the term $d\varepsilon^c$ (or $\boldsymbol{D}.d\varepsilon^c$) in equation (11) can be regarded as an initial strain (or initial stress) in the standard finite element formulation. This term can be included in the right hand side force vector, f_r, in the coupled finite element equations.

2.2 Coupled finite element formulation

The fully coupled finite analysis of consolidation has been described previously in the literature (see for example, Small *et al*, 1976). The governing system of equation may be written as:

$$\begin{pmatrix} \boldsymbol{K} & -\boldsymbol{L}^T \\ -\boldsymbol{L} & -\Delta t.\beta.\boldsymbol{\Phi} \end{pmatrix} \begin{pmatrix} \Delta\delta \\ \Delta v \end{pmatrix} = \begin{pmatrix} f_r \\ f_p \end{pmatrix} \tag{12}$$

where δ represents the nodal displacements, v denotes the nodal pore pressures, $\boldsymbol{K}$ is the stiffness matrix, $\boldsymbol{L}$ is the coupling matrix, β is an integration constant, $\boldsymbol{\Phi}$ is the flow matrix, f_p are the flow terms, and f_r is the vector of body forces and surface tractions, which includes the initial strains due to cyclic loading.

It is assumed that the process of application of wave loads on the system is so slow that the associated dynamic effects do not change the results of analysis significantly and thus may be ignored.

2.3 Finite element program

A semi-analytical approach in finite element method has been used to develop a quick and efficient finite element program. The program has the capability of three dimensional consolidation analysis. The formulation of the finite element program is based on the assumption that the field quantities such as displacements and pore pressure can be given by their discrete Fourier representation. In this method advantage is taken of the axi-symmetric nature of the problem geometry, and only one wedge from a cylinder of the soil-foundation media is modelled (Fig. 3). Instead of solving a very large number of algebraic equations, a smaller number of equations arising from a substitute problem will be solved (Taiebat, 1998). This method reduces the computational time below 5% of the time required for a standard three dimensional finite element analysis (Lai and Booker, 1991).

3 STEPS IN THE LIQUEFACTION ANALYSIS

In the liquefaction analysis, the duration of the storm is divided into a number of wave parcels. Within each parcel, the waves are assumed to be of equal height and the cyclic loads they induce to the foundation have the same amplitude. Each parcel is further divided into small time steps, of length Δt, which may include one wave or several waves.

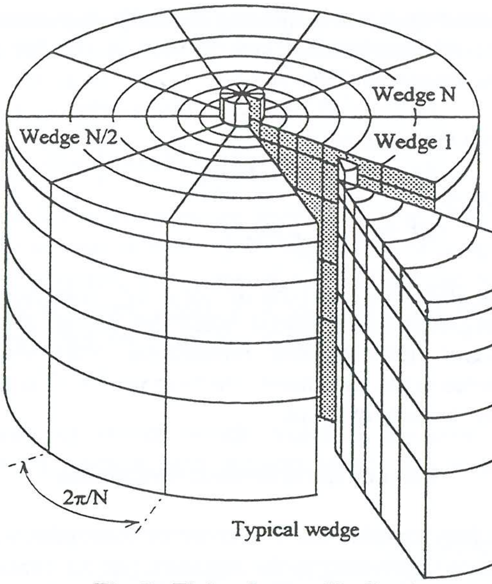

Fig. 3 : Finite element idealization

At the beginning of each time step, the pore pressure generated by the cyclic loads acting during the time interval Δt is calculated. This can be achieved by the knowledge of the number of cyclic loads applied to the foundation during the time interval, the cyclic stress ratio, q_{cyc}/p', and the experimental data such as those presented in Fig. 1 and equations (1) and (2). The effects of cyclic loads are then incorporated in the finite element program, using equation (10). The problem is then solved by computing the dissipation of pore pressure that is generated within the time increment being considered. The analysis is continued by marching forward in time, computing the pore pressure generated by cyclic loading and the dissipation by soil consolidation, until all parcels of wave loading have been considered and the end of storm is reached.

The initial mean and deviatoric stresses, p' and q, and cyclic deviatoric stress, q_{cyc}, are evaluated by the program whenever any change in loading occurs during the storm.

4 ILLUSTRATIVE EXAMPLE

Prediction of the liquefaction potential of the seabed soil around a single pile subjected to cyclic loading was investigated as an illustration of the proposed method. The finite element program and the procedure described in the previous section have been used in the analysis.

4.1 Definition of the problem

A single pile with a length of *80m* and a diameter of *2m* embedded in calcareous sand was considered. The Young's modulus of the pile is *200GPa*. The soil layer was assumed to be essentially elastic. The soil Young's modulus was defined as $E'=1.0\ z$ (*MPa*), where z is the depth in metres below the mudline. The soil has a coefficient of permeability of $k=5.4\times10^{-6} m/sec$, a submerged unit weight of $\gamma_{sub}=7kN/m^3$, and a coefficient of in situ lateral pressure of $K_o=0.3$. The cyclic properties of the calcareous soil are described by Fig.1, equations (1) and (2).

The magnitude of the ambient axial and lateral loads on th pile are *25,000 kN* and *2,000 kN*, respectively. Also mudmat with a radius of *4m* exerts a uniform pressure *100kPa* on the surface of the soil. It is assumed that th ambient loads remain constant during the storm.

The storm loading considered in this analysis has bee generated for cyclones with *100* and *10,000* year retur periods. The wave composition and their duration are show in Table 1. The storm was assumed to have a simple wav load composition, increasing in magnitude from zero to it maximum value at the peak of the storm, and reducin gradually to zero after the peak. Fig. 4 shows the storr histogram adopted in this analysis. The peak of storm for *10* and *10,000* year return period is *24hrs* and *20hrs* after th start of the storms, respectively.

It was assumed that the storms generate only a lateral cyclic loa on the pile. The cyclic loads, H_{cyc}, is a function of wave height i.e. $H_{cyc}=0.268h^{2.6}$ (*kN*), where h is the wave height in metres.

Table 1 : Composition of wave heights for storms

Wave Height (*m*)	Period (*sec.*)	No. of waves	
		100 yr.	*10,000 yr.*
0 - 1	4.6	4254	4227
1 - 2	5.8	3490	3196
2 - 3	7.0	3054	2012
3 - 4	8.2	2290	1514
4 - 5	9.4	1964	1125
5 - 6	10.6	1310	931
6 - 7	10.7	982	717
7 - 8	10.9	796	680
8 - 9	11.1	644	525
9 - 10	11.3	436	467
10 - 11	11.5	306	363
11 - 12	11.7	208	381
12 - 13	11.9	142	284
13 - 14	12.1	88	228
14 - 15	12.3	54	140
15 - 16	12.5	34	118
16 - 17	12.7	20	120
17 - 18	12.9	10	66
18 - 19	13.1	6	34
19 - 20	13.4	4	20
20 - 21	13.6	2	17
21 - 22	13.6	0	19
21.8	**13.8**	**1**	0
22 - 23	14.0	0	13
23 - 24	14.2	0	7
24 - 25	14.4	0	4
25- 26	14.6	0	4
26 - 27	14.8	0	1
28.4	**15.0**	0	**1**

4.2 Results of the analysis

Excess pore pressures were predicted around the pile during the storm. For the storm with *100* year return period, the magnitude of the pore water pressure is not significant during the first *13* hours of the storm. Application of larger waves generates increasing excess pore pressures up to the peak of the storm, after which the excess pore pressures steadily reduce to zero. Similar trends can be observed during the analysis for *10,000yr.* storm. The variations of the maximum values of the excess pore pressures generated during the storms are shown in Fig. 5. The maximum pore pressure in the soil is not sustained for more than *30* minutes.

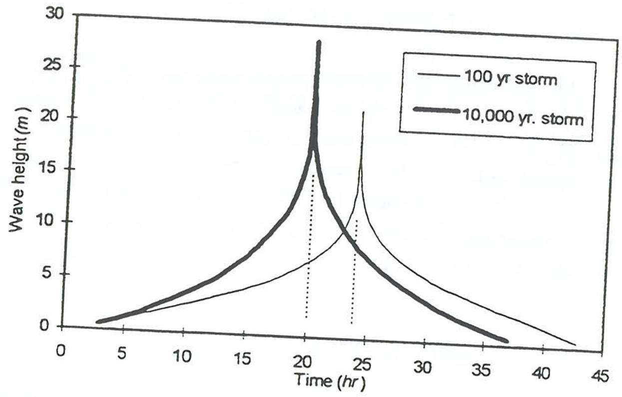

Fig. 4 : Storm histogram

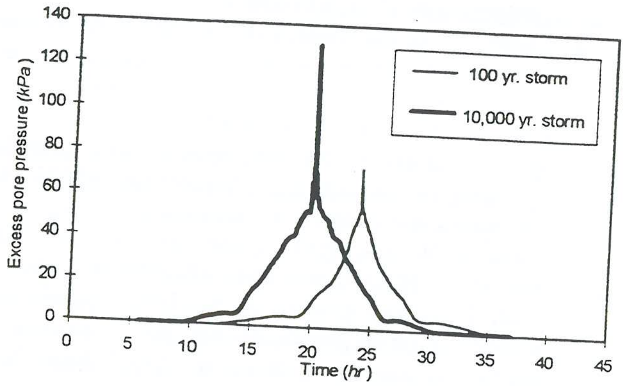

Fig. 5 : Variations of the maximum excess pore pressure during the storms

The distribution of predicted excess pore pressure in the vertical plane containing the applied lateral load, at the peak of storm, is illustrated in Fig. 6 and Fig. 7, for the *100yr.* and *10,000yr.* storms, respectively. These figures show that the zone of high pore pressure is limited to a small area around the pile. Application of the *10,000yr.* storm loading results in a wider and deeper zone of excess pore pressure around the pile, as expected.

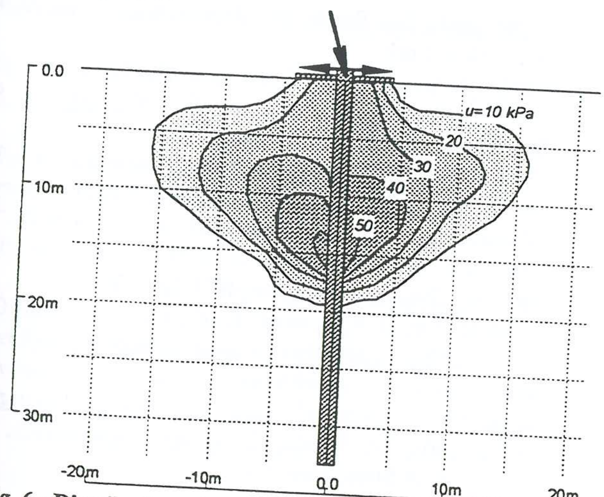

Fig. 6 : Distribution of excess pore pressure for the storm with *100* year return period at the storm peak

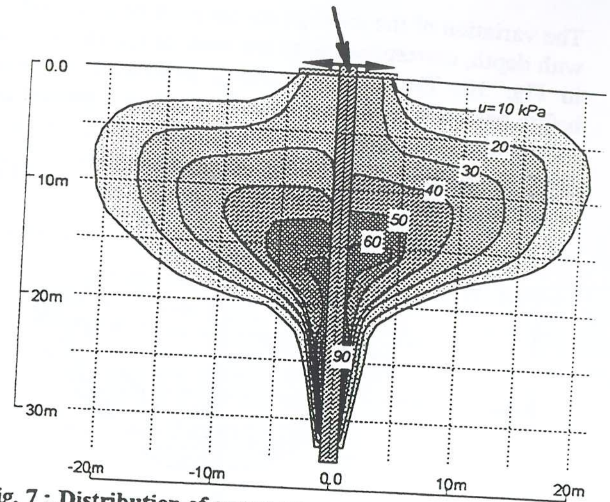

Fig. 7 : Distribution of excess pore pressure for the storm with *10,000* year return period at the storm peak

Representative values of pore pressure have been obtained by averaging the pore pressures in a region adjacent to the pile to a distance of four diameters from the pile and over the horizontal angular range from the direction of applied lateral load to *90°* from this direction. The variation of these average values with depth at the peak of the storm is shown in Fig. 8.

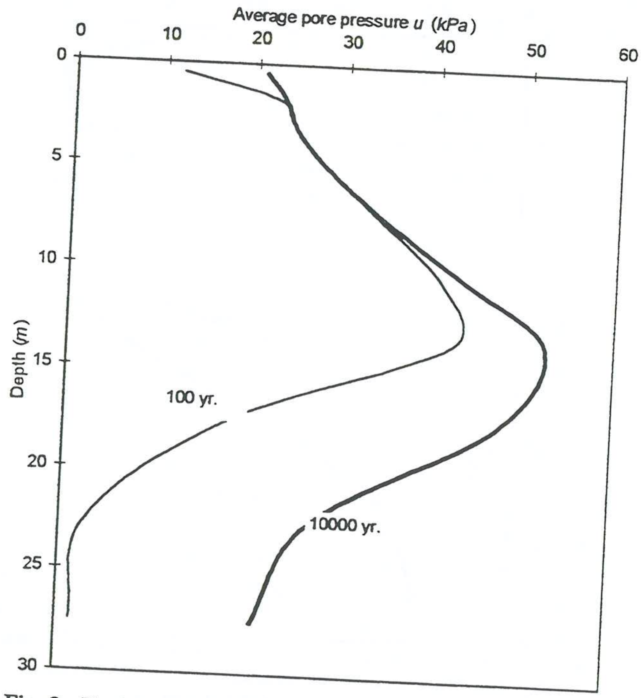

Fig. 8 : Variation of the average excess pore pressure with depth at the strom peak

If liquefaction is deemed to occur when the value of pore pressure reaches the same magnitude as the mean initial stress, then the results of analyses for both storms indicate the development of liquefaction in the soil around the pile. The extent of liquefied zones in the vertical plane of the applied lateral load is shown in Fig. 9. It can be seen that the liquefied zones in this section extend to a depth of *12.5m* for the *100yr.* storm and *17m* for the *10,000yr.* storm.

The variation of the average excess pore pressure ratio, *u/p'*, with depth, corresponding to the peak of the storm, is shown in Fig. 10. The same averaging procedure as explained before has been used. Fig. 10 indicates that a general zone of liquefaction covers the top layer of the soil, which has a thickness of about *8m* for the *100yr.* storm and *13m* for the *10,000yr.* storm.

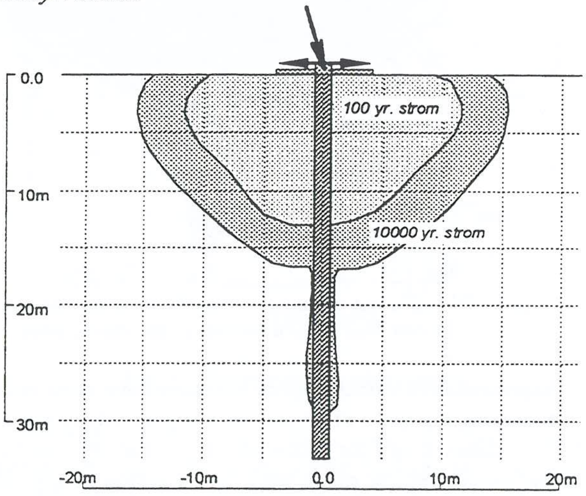

Fig. 9 : Liquefied zone at the storm peak

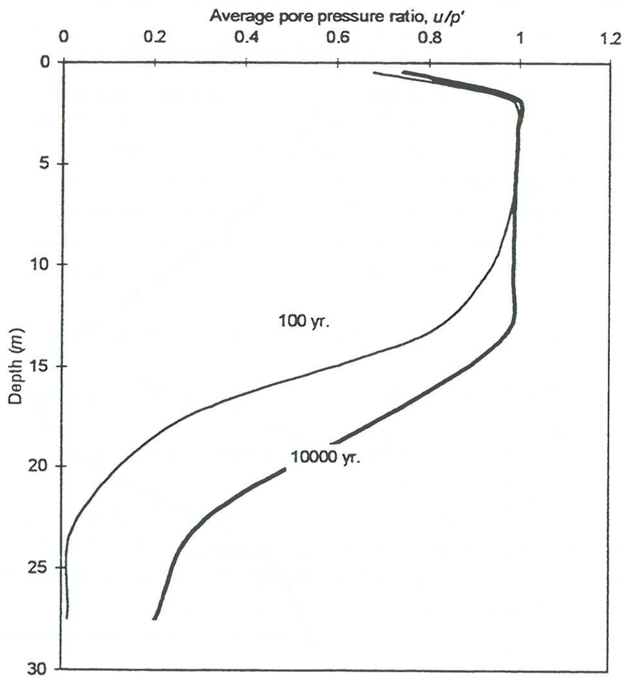

Fig. 10 : Variation of the average excess pore pressure ratio with depth at the storm peak

5 CONCLUSION

A method of analysis was presented which can be used for three dimensional liquefaction analysis of offshore foundations subjected to cyclic wave loading. The method was used to analyse a hypothetical single pile subjected to cyclic loading. The results of study on the pile show that the possibility of liquefaction of the soil around the top section of the pile is high. Therefore, the resistance of that part of the soil should be ignored in the design procedures.

6 ACKNOWLEDGMENT

The material published herein is a part of Ph.D. research program currently undertaking by the writer. The supervision of Prof. John Carter during the course of studies is greatly appreciated. The support provided by Centre for Geotechnical Research (CGR) and Centre for Offshore Foundation System (COFS) at the University of Sydney is also acknowledged.

7 REFERENCES

1. Bjerrum, L. (1973) "*Geotechnical problems involved in foundations of structures in the North Sea*", Geotechnique, 23, 3, 319-358
2. Chugh, A. K. and Thun, J. L. V. (1985) "*Pore pressure response analysis for earthquakes*". Canadian Geotech. J., 22, 466-76
3. Finn, W. D. L., Lee, K. W. and Martin, G. R. (1976) "*An effective stress model for liquefaction*", Liquefaction Problems in Geotechnical Engineering, ASCE, Annual convention and exposition, Philadelphia.
4. Kaggwa, W. S. (1988) "*Cyclic behaviour of carbonate sediments*", Ph.D. thesis, The University of Sydney.
5. Lai, J. Y. and Booker, J. R. (1991) "*Application of discrete Fourier series to the finite element stress analysis of axi-symmetric solids*", Int. J. Num. Methods in Engineering, 31, 619-47
6. Lee, K. L. and Focht, J. A. (1975) "*Liquefaction potential at Ekofisk tank in North Sea*", J. Geotech. Division, ASCE, GT1, 1, 18
7. Rahman, M. S., Seed, H. B. and Booker, J. R. (1977) "*Pore pressure development under offshore gravity structures*", J. Geotech. Division, ASCE, GT12, 103, 1419-36
8. Seed, H. B. and Idriss, I. M. (1982) "*On the importance of dissipation effects in evaluating pore pressure changes due to cyclic loading*", Soil mechanics-Transient and cyclic loads, Ed. Pande and Zienkiewicz, John Wiley & Sons, New York
9. Small, J. C., Booker, J. R. and Davis, E. H. (1976) "*Elasto-plastic consolidation of soil*", Int. J. Solids Structures, 12, 431-88
10. Taiebat, H. A. (1998) "*Numerical analysis of offshore foundations*", Ph.D. thesis, The University of Sydney
11. Zienkiewicz, O. C. and Taylor, R. L. (1989) "*Semi-analytical finite element processes*", The finite element method, Chapter 6, McGraw-Hill, New York
12. Zienkiewicz, O. C., Leung, K. H., Hilton, E. and Chang, C. T. (1982) "*Liquefaction and permanent deformation under dynamic conditions- Numerical solution and constitutive relations*", Soil Mechanics-Transient and cyclic loads, Ed. Pande, G. N. and Zienkiewicz, O. C., John Wily & Sons, New York